applied sciences

MDPI

Article

Design Theory and Application of Reinforcement for Existing Slab Culverts Through the Additional Deck Slab

Zhijie Jiang [1], Junxi Ning [2], Huaxing Chen [2] and Yongjiang Shen [2,*]

[1] Guangxi Jiaojian Engineering Construction Group Co., Ltd., Nanning 530000, China; m13397706629@163.com
[2] School of Civil Engineering, Central South University, Changsha 410075, China; 244812343@csu.edu.cn (J.N.); 244811024@csu.edu.cn (H.C.)
* Correspondence: 209059@csu.edu.cn

Featured Application

The proposed reinforcement method can be applied to existing slab culverts requiring capacity enhancement in highway widening projects. By combining an additional deck slab with a grouted steel pipe pile-supported composite foundation, it provides a rapid, cost-effective solution with minimal traffic disruption. The developed design approach can support the optimization of reinforcement parameters in practical engineering applications.

Abstract

To address the insufficient bearing capacity of existing slab culverts under increased fill heights in highway widening projects, a reinforcement method integrating an additional deck slab with a grouted steel pipe pile-supported composite foundation is proposed. A segmented elastic foundation beam model is developed to derive the analytical solution for slab deflection and calculate the load acting on the culvert roof. A three-dimensional finite element model is established in Abaqus, in which the soil is modeled using the Mohr–Coulomb elastoplastic constitutive model to investigate the effects of pile arrangement, pile diameter, pile length, pile spacing, and fill height on reinforcement performance. The results show that culvert displacement and stress decrease with reduced pile spacing and increased pile diameter and pile length, while the best reinforcement performance among the investigated cases is achieved when the piles extend 4 m below the culvert base slab Field tests from the Beijing–Hong Kong–Macao Expressway widening project demonstrate the applicability of the proposed reinforcement method and show that pressure grouting increases the coefficient of subgrade reaction by 7–10%. Based on theoretical and field investigations, recommended reinforcement parameters are proposed for a representative culvert. The proposed method provides an efficient solution for culvert reinforcement in highway widening projects.

Keywords: highway widening; additional deck slab reinforcement; elastic foundation beam; composite foundation; field test

Check for updates

Academic Editor: Paulo Santos

Received: 12 June 2026
Revised: 13 July 2026
Accepted: 20 July 2026
Published: 21 July 2026

1. Introduction

Highway bridges and culverts, as important components of transportation infrastructure and hydraulic engineering, perform critical functions such as drainage, flood control, and traffic passage [1]. However, constrained by the technical and economic conditions at the time of construction, the project suffered from inherent deficiencies, including inadequate design standards, insufficient construction management, outdated equipment, and limited material performance, which ultimately resulted in multiple construction defects [2]. In addition, the implementation of highway widening projects has altered the elevation of certain sections, resulting in increased embankment fill above some existing bridges and culverts, thereby further increasing their load [3]. Therefore, appropriate measures are required to improve the bearing capacity of existing structures and mitigate the adverse effects of additional loads.

For the insufficient bearing capacity of existing culverts, commonly used rehabilitation methods include lining reinforcement [4], corrugated steel lining [5], sprayed UHPC reinforcement [6], and staged demolition and reconstruction after excavation. However, these methods exhibit various limitations in practical applications: internal lining reinforcement improves structural stiffness but significantly reduces clearance [7]; corrugated steel lining requires high construction precision and exhibits limited capability in controlling crown settlement [8]; sprayed UHPC reinforcement provides high strength and durability but involves extremely high material costs and strict construction conditions [9]; staged demolition and reconstruction require complete traffic interruption and involve multiple processes such as excavation, demolition, reconstruction, curing, and backfilling, resulting in long construction periods, high costs, and significant environmental disturbance.

In addition to these rehabilitation techniques, previous studies have investigated load-relieving systems, load-distribution methods, and foundation improvement techniques to reduce the load acting on buried culverts or enhance the bearing capacity of the supporting ground [10–12]. Load-relieving systems primarily reduce the earth pressure transmitted to culverts by modifying the load-transfer path within the embankment, whereas foundation improvement techniques improve the stiffness of the supporting soil and strengthen soil–structure interaction. Existing culvert assessment methods generally evaluate structural performance through analytical approaches, numerical simulations, or field measurements under different loading conditions [13–15]. Although these methods have demonstrated satisfactory performance under specific engineering conditions, they generally focus on either load redistribution or foundation enhancement individually, and relatively limited attention has been paid to their combined application for existing slab culverts subjected to increased embankment loads in highway widening projects.

For highway widening projects, which typically face constraints such as limited construction time, strict traffic maintenance requirements, and heavy workloads, it is difficult for conventional reinforcement methods to achieve an appropriate balance among construction efficiency, cost, and structural performance. To address this research gap and meet the practical demands of highway widening projects, the objective of this study is to develop a composite reinforcement method integrating an additional deck slab with a grouted steel pipe pile-supported composite foundation. Unlike conventional load-relieving systems or foundation improvement methods applied separately, the proposed method simultaneously redistributes embankment loads and enhances foundation stiffness, thereby improving the bearing capacity of existing slab culverts while minimizing construction time, traffic disruption, and environmental impact. A segmented Winkler foundation beam model, three-dimensional finite element analysis, and field tests are employed to investigate the reinforcement mechanism and evaluate the performance of the proposed method. The outcomes of this study are expected to provide both a theoretical basis for reinforcement design and practical guidance for the rehabilitation of existing slab culverts in highway widening projects.

https://doi.org/10.3390/app16147318

2. Design and Calculation Method for Additional Deck Slab Reinforcement

Considering the limitations of conventional reinforcement methods in terms of structural performance, economy, and construction duration, a reinforcement method involving an additional deck slab is proposed (see Figure 1).

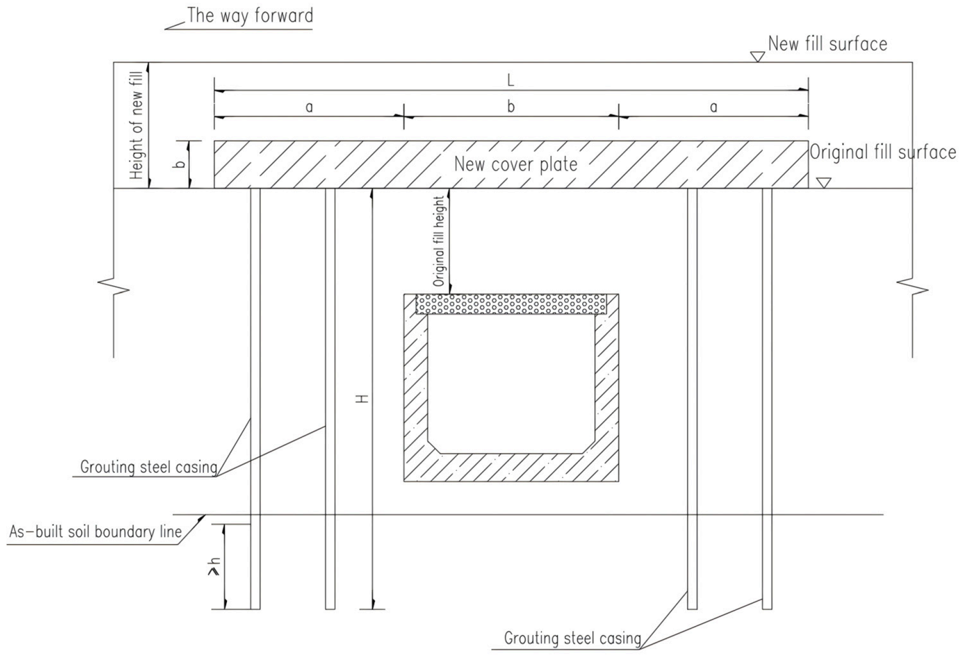

Figure 1. Schematic diagram of the additional deck slab reinforcement method.

In the design calculation, the midspan of the additional deck slab is simplified as an elastic foundation beam, while grouted steel pipe piles are installed in the soil on both sides to form a composite foundation [16–19]. Accordingly, the foundation coefficient is defined in a piecewise manner: the composite foundation sections at both ends are assigned a coefficient of k1, while the middle section of the in situ soil is assigned a coefficient of k2. Each segment is analyzed using a Winkler foundation model with a constant coefficient to derive the general solution for deflection. By applying continuity conditions of deflection, rotation, bending moment, and shear force between segments, a system of equations is established to determine the integration constants, thereby obtaining the analytical solution for the deflection of the entire beam.

On this basis, the final displacement of the soil beneath the slab is determined by superposition of the composite foundation settlement and the slab deflection, and the load acting on the culvert roof is back-calculated. The proposed method is evaluated by comparing the load acting on the existing culvert before and after reinforcement.

2.1. Composite Foundation Calculation

According to the Technical Code for Composite Foundation (GB/T 50783-2012) [20], the settlement of a composite foundation consists of the compressive deformation of the cushion layer, the reinforced composite soil layer, and the underlying soil layer. When the cushion deformation is small and essentially completed during construction, it may be neglected. The composite foundation settlement can be calculated as:

$$s = s_1 + s_2 \tag{1}$$

where s_1 denotes the compressive deformation of the reinforced composite soil layer (mm); s_2 denotes the compressive deformation of the underlying soil layer (mm).

The compressive deformation of the reinforced composite soil layer for rigid pile composite foundations can be calculated as:

$$s_1 = \psi_p \frac{Ql}{E_p A_p} \tag{2}$$

where Q denotes the additional load at the pile head (kN); l denotes the pile length (mm); E_p denotes the elastic modulus of the pile material (kPa); A_p denotes the cross-sectional area of a single pile (m^2); ψ_p denotes the empirical coefficient for pile compression.

The compressive deformation of the underlying soil layer can be calculated as:

$$s_2 = \psi_{s2} \sum_{i=1}^{n} \frac{\Delta p_i}{E_{si}} l_i \tag{3}$$

where Δp_i denotes the average additional stress increment of the i-th soil layer (kPa); l_i denotes the thickness of the i-th layer (mm); E_{si} denotes the compression modulus of the i-th layer (kPa); ψ_{s2} denotes the empirical coefficient.

2.2. Calculation of the Additional Deck Slab

The elastic foundation beam model is used to analyze the additional deck slab. The piecewise definition of the foundation coefficient directly corresponds to the empirical reinforcement layout, where k_1 represents the enhanced stiffness of the grouted steel pipe pile composite foundation, and k_2 denotes the subgrade reaction of the unreinforced in situ soil. The foundation coefficient can be expressed as:

$$k = \begin{cases} k_1, 0 \le x \le \mathrm{a} \\ k_2, \mathrm{a} < x < \mathrm{a} + \mathrm{b} \\ k_1, \mathrm{a} + \mathrm{b} \le x \le L \end{cases} \tag{4}$$

where a denotes the length of the ground improved by steel-tube grouting piles on both sides; b denotes the span of the culvert; L denotes the total length of the model.

The governing equation is:

$$EI \frac{d^4 \omega}{dx^4} + k\omega(x) = q(x) \tag{5}$$

For a uniformly distributed load, the particular solution is:

$$\omega_p = \frac{q}{k} \tag{6}$$

The governing equation applies to each segment, and considering symmetry, the general solutions are given as:

For $0 \le x \le \mathrm{a}$:

$$\omega_1(x) = e^{\beta_1 x}[A_1 \cos(\beta_1 x) + B_1 \sin(\beta_1 x)] + e^{-\beta_1 x}[C_1 \cos(\beta_1 x) + D_1 \sin(\beta_1 x)] + \frac{q}{k_1} \tag{7}$$

For $\mathrm{a} < x \le \frac{L}{2}$:

$$\omega_2(x) = e^{\beta_2 x}[A_2 \cos(\beta_2 x) + B_2 \sin(\beta_2 x)] + e^{-\beta_2 x}[C_2 \cos(\beta_2 x) + D_2 \sin(\beta_2 x)] + \frac{q}{k_2} \tag{8}$$

https://doi.org/10.3390/app16147318

where A, B, C, D are coefficients; $\beta_1 = \left(\frac{k_1}{4EI}\right)^{\frac{1}{4}}$, $\beta_2 = \left(\frac{k_2}{4EI}\right)^{\frac{1}{4}}$; E denotes the elastic modulus of the beam; I denotes the moment of inertia of the cross-section.

The boundary conditions are specified as follows: at the left end of the beam, the displacement and rotation are both zero, corresponding to a fixed-end constraint; at the right end, the rotation and shear force are both zero. At the interface points between segments, continuity conditions of displacement, rotation, bending moment, and shear force are satisfied. According to the Winkler beam on elastic foundation theory, the deflection and rotation of the beam attenuate exponentially with increasing distance from the point of load application. Since the length of the reinforced zone is substantially greater than its thickness, the deflection and rotation at the extremities of this segment can be safely neglected.

$$\begin{cases} \omega_1(0) = 0 \\ \omega_1'(0) = 0 \\ \omega_2'(\frac{L}{2}) = 0 \\ \omega_2'''(\frac{L}{2}) = 0 \\ \omega_1(\mathrm{a}) = \omega_2(\mathrm{a}) \\ \omega_1'(\mathrm{a}) = \omega_2'(\mathrm{a}) \\ EI\omega_1''(\mathrm{a}) = EI\omega_2''(\mathrm{a}) \\ EI\omega_1'''(\mathrm{a}) = EI\omega_2'''(\mathrm{a}) \end{cases} \tag{9}$$

The derived system of algebraic equations is inherently coupled and can be efficiently solved using a banded pentadiagonal sparse matrix solver to determine the undetermined integration constants, thereby yielding the continuous deflection along the beam. In this piecewise foundation model, instead of spatial mesh discretization, the pentadiagonal-like structure naturally arises from the localized continuity and boundary matching conditions connecting adjacent segments, where the internal forces and displacements at each interface are explicitly expressed by the constants of its neighboring segments. The calculation process is shown in Figure 2. First, the general analytical solution of the fourth-order governing differential equation is formulated for each independent foundation segment. Second, at each internal segment interface, 4 continuous matching conditions are enforced, which include the continuity of vertical displacement, rotation, bending moment, and shear force. Third, the physical boundary conditions are applied at the boundaries of the continuous beam. Fourth, because each interface condition strictly couples only the integration constants of two adjacent segments, assembling these boundary and interface algebraic equations forms a highly localized, banded, pentadiagonal-like sparse coefficient matrix. Fifth, standard matrix inversion is performed to solve the 4N constants simultaneously, which are then substituted back into the general solutions to yield the exact continuous deflection and internal forces across the entire span.

$$\frac{d^4\omega}{dx^4} \approx \frac{\omega_{i-2} - 4\omega_{i-1} + 6\omega_i - 4\omega_{i+1} + \omega_{i+2}}{(\Delta x)^4} \tag{10}$$

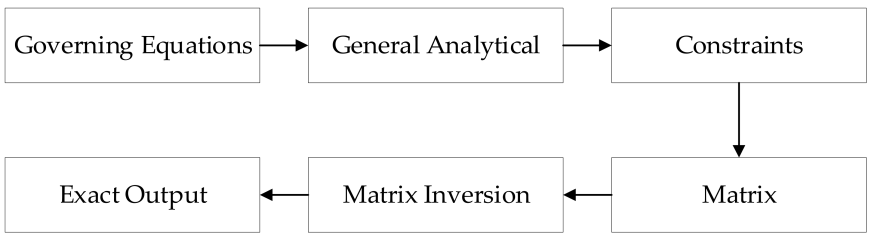

Figure 2. Calculation process.

Substituting this expression into the governing equation of the elastic foundation beam yields:

$$\frac{EI}{(\Delta x)^4}\omega_{i-2} - 4\frac{EI}{(\Delta x)^4}\omega_{i-1} + (\frac{6EI}{(\Delta x)^4} + k_i)\omega_i - \frac{4EI}{(\Delta x)^4}\omega_{i+1} + \frac{EI}{(\Delta x)^4}\omega_{i+2} = q_i \tag{11}$$

Under the Winkler foundation assumption, the slab is modeled as an elastic foundation beam supported by independent linear springs, with:

$$f = ky \tag{12}$$

where y denotes the vertical displacement of the beam, and k denotes the coefficient of subgrade reaction.

Considering the safety factor, the total displacement is:

$$\omega_z = \mu \cdot \omega_q(\frac{L}{2}) \tag{13}$$

To establish a mathematically rigorous relationship for the load transition from the additional deck slab to the existing culvert, the principle of deformation compatibility within the intervening soil medium is employed. Under vehicular and overburden loads, the continuous vertical deflection of the additional slab is denoted as w(x). According to the Winkler foundation framework within the mid-span segment, the contact pressure at the soil–slab interface is proportional to the local soil compression. To quantitatively justify the fixed-end boundary condition, the characteristic parameter of the Winkler foundation beam was evaluated as $\beta_1 = \left(\frac{k_1}{4EI}\right)^{\frac{1}{4}}$, where k_1 = 135 MPa/m is the subgrade coefficient of the pile-reinforced zone, E = 30 GPa is the elastic modulus of the deck slab, and h = 0.4 m is the slab thickness. This yields β ≈ 0.515 m^{-1}, corresponding to a characteristic length of 1/β ≈ 1.94 m. Given the length of the reinforced zone a = 4 m (accounting for the lateral diffusion of the grouted zone beyond the nominal pile spacing), the deflection decay function $e^{-\beta x}(\cos\beta x + \sin\beta x)$ has attenuated to approximately 5.25% of its characteristic amplitude at the assumed fixed-end location, confirming that the fixed-end approximation introduces only a small, quantifiable error consistent with standard practice in Winkler beam analysis. Consequently, the vertical compression of the subgrade fill matches the downward deflection of the additional slab exactly. Through in situ plate load tests, incremental loading is applied and the corresponding settlements are measured to determine the coefficient of subgrade reaction k, thereby obtaining the load acting on the underside of the midspan of the additional deck slab as follows:

$$F_b = k \cdot \omega_z \tag{14}$$

On this basis, the external forces acting on the soil between the existing top slab of the culvert and the additional deck slab, together with the self-weight of the soil, yield the total load on the culvert roof. This load should not exceed that under the unreinforced condition.

3. Numerical Analysis

3.1. Introduction to the Numerical Analysis Model

To investigate the reinforcement mechanism of the proposed system and evaluate the influence of key design parameters, a three-dimensional finite element model was established in Abaqus. In the numerical model, the soil was represented using the Mohr–Coulomb elastoplastic constitutive model, whereas the concrete culvert, the additional deck slab, and the grouted steel pipe piles were modeled as linear-elastic materials.

Therefore, the nonlinear behavior considered in the analysis is limited to the constitutive response of the soil. According to the structural characteristics of the system, appropriate geometric simplifications were adopted in the finite element model. As shown in Figure 3, the principal geometric parameters of the model are as follows: the soil dimensions (height $\times$ width $\times$ thickness) are taken as 14 m $\times$ 18 m $\times$ 2 m; the culvert external dimensions include width 2 m, height 2 m, wall thickness 0.5 m, culvert base slab thickness 0.6 m, and original deck slab thickness 0.4 m; the thickness of the additional deck slab is 0.3 m.

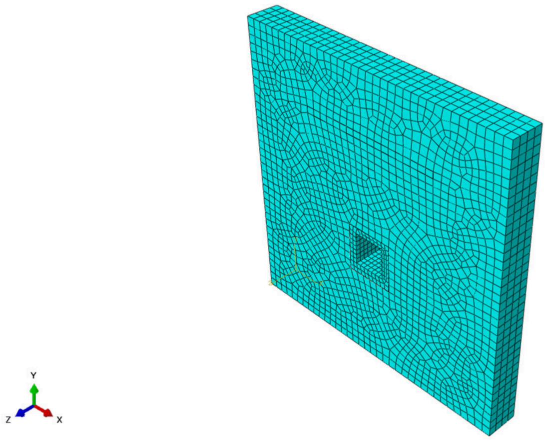

Figure 3. Finite element model.

The boundary conditions of the model are specified as follows: the bottom surface and lateral boundaries are constrained in the normal direction, while the top surface is defined as a free boundary. The initial stress field is established using geostatic equilibrium analysis. The material parameters used in the numerical simulation are summarized in Table 1. The soil properties were primarily obtained from the geotechnical investigation report of the project site, while the elastic properties of concrete and steel were adopted in accordance with the Code for Design of Concrete Structures (GB 50010-2010, 2015 Edition) and the Standard for Design of Steel Structures (GB 50017-2017) [21,22]. Typical values reported in the geotechnical engineering literature were adopted where necessary. The pile–soil interaction was simplified using an embedded-region constraint, in which the grouted steel pipe piles were embedded within the surrounding soil elements without allowing relative slip or separation at the pile–soil interface. This treatment is consistent with common practice in composite-foundation numerical studies that focus on the overall deformation and stress response of the reinforced system rather than local interface slippage. The load was applied in a single step to represent the final in-service condition after reinforcement, rather than simulating the sequential construction process; this simplification is considered acceptable given that the present study focuses on the long-term operational performance of the reinforced culvert rather than construction-induced transient effects. The soil was modeled using the Mohr–Coulomb constitutive model with effective-stress strength parameters corresponding to the fully consolidated, drained condition of the embankment fill, consistent with the long-term settlement and loading state considered in this study. The mesh type is designated as C3D8R. The global mesh size is set to 0.5 m, except for the culvert structure itself, which is refined to 0.3 m. To demonstrate mesh convergence, finite element simulations were conducted using three different mesh sizes, specifically 0.5 and 2 times the current baseline dimensions. The numerical results indicate that the vertical stress of the culvert top slab varies by only 1.15% and 4.67%, respectively. This clearly demonstrates that the mesh density adopted in the present study is sufficient to ensure mesh-independent results.

Table 1. Table of Calculation Parameters.

Materials	ρ/kg/m^3	E/Mpa	μ	C/kPa	φ/°
Soil	2100	20	0.3	10	20
Concrete	2500	30,000	0.3	–	–
Steel	7850	210,000	0.3	–	–

3.2. Parameter Combination and Results Analysis

A reference case was established for the parametric study with an inner-side pile distance of 1 m from the culvert, a pile diameter of 89 mm, a pile length extending 2 m below the culvert base slab, and a pile spacing of 2 m. To clearly evaluate the influence of individual design parameters on the reinforcement performance, a single-factor analysis was adopted. Parametric numerical models were subsequently generated by varying one parameter at a time while keeping all remaining parameters identical to those of the reference case, as summarized in Table 2. This approach enables the individual effects of key design variables to be systematically identified while avoiding interference from simultaneous changes in multiple parameters. The effects of pile group arrangement, pile diameter, pile length, and pile spacing on the reinforcement performance were therefore systematically investigated.

Table 2. Calculation Parameters.

<table>
<tr><th>Combination of Parameters</th><th>Pile Group Arrangement (m)</th><th>Pile Diameter (mm)</th><th>Pile Length (m)</th><th>Pile Spacing (m)</th></tr>
<tr><td>1</td><td>Two rows of piles, each 1 m from the edge of the culvert and the cover plate</td><td rowspan="2">89</td><td rowspan="2">extending 2 m below the culvert base slab</td><td rowspan="2">2</td></tr>
<tr><td>2</td><td>Two rows of piles, each 0.5 m from the edge of the culvert and the cover plate</td></tr>
<tr><td>3</td><td rowspan="3">Two rows of piles, each 1 m from the edge of the culvert and the cover plate</td><td>75</td><td rowspan="3">extending 2 m below the culvert base slab</td><td rowspan="3">2</td></tr>
<tr><td>4</td><td>89</td></tr>
<tr><td>5</td><td>100</td></tr>
<tr><td>6</td><td rowspan="3">Two rows of piles, each 1 m from the edge of the culvert and the cover plate</td><td rowspan="3">89</td><td>terminating at the culvert base slab</td><td rowspan="3">2</td></tr>
<tr><td>7</td><td>extending 2 m below the culvert base slab</td></tr>
<tr><td>8</td><td>extending 4 m below the culvert base slab</td></tr>
<tr><td>9</td><td>Five rows of piles, each 1 m from the edge of the culvert and the cover plate</td><td rowspan="3">89</td><td rowspan="3">extending 2 m below the culvert base slab</td><td>0.5</td></tr>
<tr><td>10</td><td>Three rows of piles, each 1 m from the edge of the culvert and the cover plate</td><td>1</td></tr>
<tr><td>11</td><td>Two rows of piles, each 1 m from the edge of the culvert and the cover plate</td><td>2</td></tr>
</table>

To investigate the influence mechanism of different parameters on the strengthening effectiveness, numerical simulations were first performed using the single-factor method, and the culvert deck displacement, vertical stress of the deck slab, and lateral stress of the side walls were selected as key indicators. Based on the results shown in Figure 4, the variation trends of these indicators were systematically analyzed to clarify the effects of each parameter.

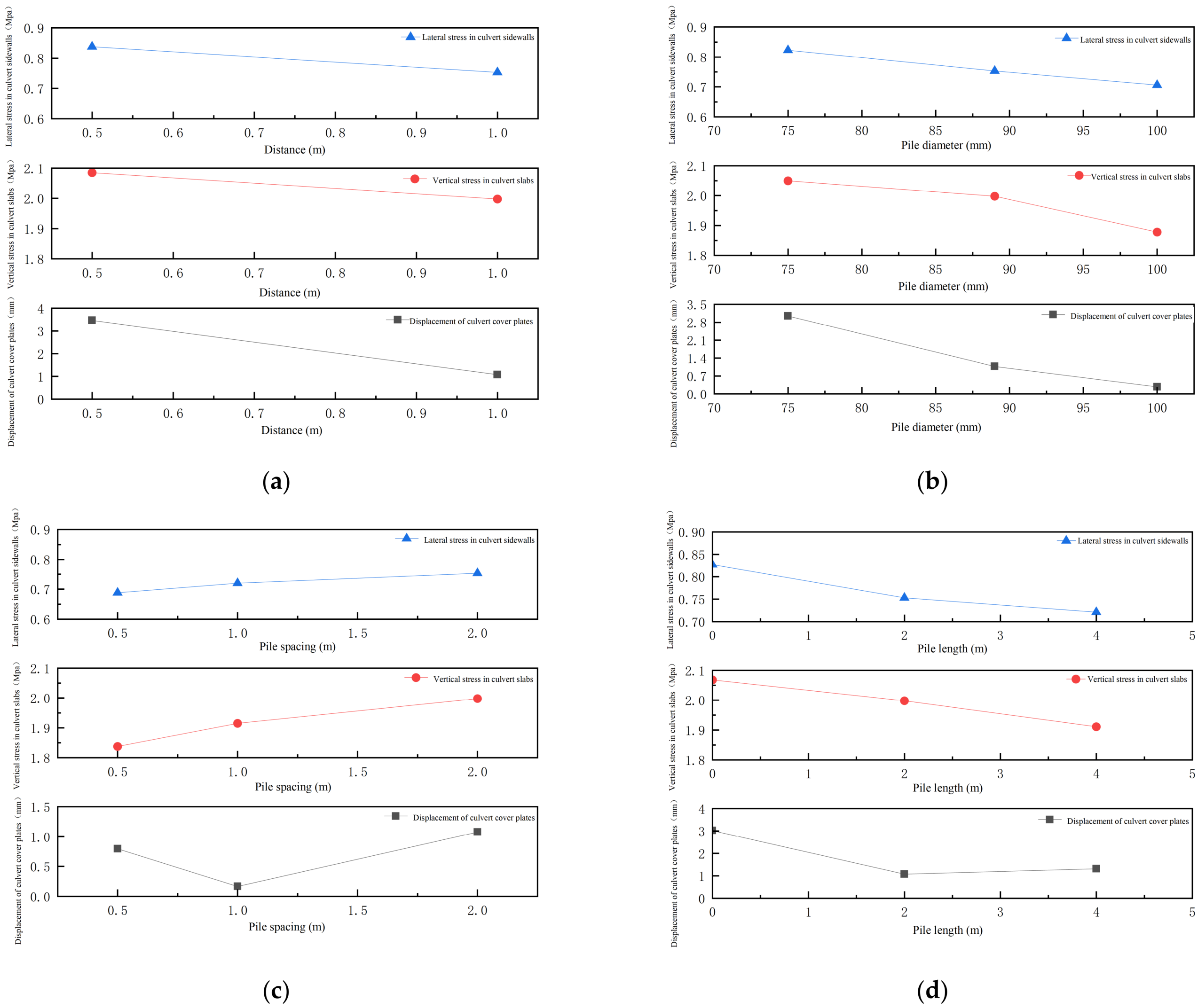

Figure 4. Effects of additional deck slabs under different parameters: (**a**) Distance; (**b**) Pile diameter; (**c**) Pile spacing; (**d**) Pile length.

Through a comparative analysis of the key parameters, the results indicate that the displacement and stress responses of the culvert structure decrease as the inner-side distance of the reinforcement system decreases, the pile diameter and pile length increase, and the pile spacing decreases (i.e., the number of piles increases). Specifically, the deck displacement, vertical stress of the additional deck slab, and lateral stress of the side walls all decrease with decreasing inner-side distance and increasing pile diameter. Increasing pile length effectively reduces both vertical and lateral stresses. When the piles extend 2 m or 4 m below the culvert base slab, the reinforcement performance is better than that achieved with piles terminating at the culvert base slab. Furthermore, reducing pile spacing to increase the number of piles is also beneficial for controlling culvert stresses.

The numerical results show that increasing pile length can further reduce the structural response and improve the reinforcement performance. However, the improvement gradually decreases with the continuous increase in pile length, while the additional material consumption continues to increase. This indicates that the relationship between reinforcement efficiency and construction input is nonlinear. Therefore, the selection of pile length should consider both the required reinforcement performance and construction economy. For the engineering case investigated in this study, the selected pile length provides a reasonable balance between structural improvement and additional reinforcement cost.

To evaluate whether the simultaneous variations in reinforcement parameters induce coupling effects on the structural response, a multi-variable analysis is conducted based on a comprehensive matrix of 27 simulation cases. Three key geometric parameters are evaluated concurrently: pile length (0, 2, 4 m), pile diameter (75, 89, 100 mm), and pile spacing (0.5, 1, 2 m). Figure 5 illustrates the variation of the vertical stress on the culvert top slab across different parameter combinations. It can be observed that while each individual factor exerts a pronounced primary effect on the structural stress, their mutual interactions are highly uncoupled. Specifically, increasing the pile length from 0 to 4 m or enlarging the pile diameter from 75 to 100 mm consistently and monotonically decreases the vertical stress. More importantly, the stress reduction curves associated with varying the pile spacing remain essentially parallel across all tested combinations of pile lengths and diameters. Therefore, the optimization of the reinforcement layout can be reliably guided by superimposing the independent main effects of individual parameters.

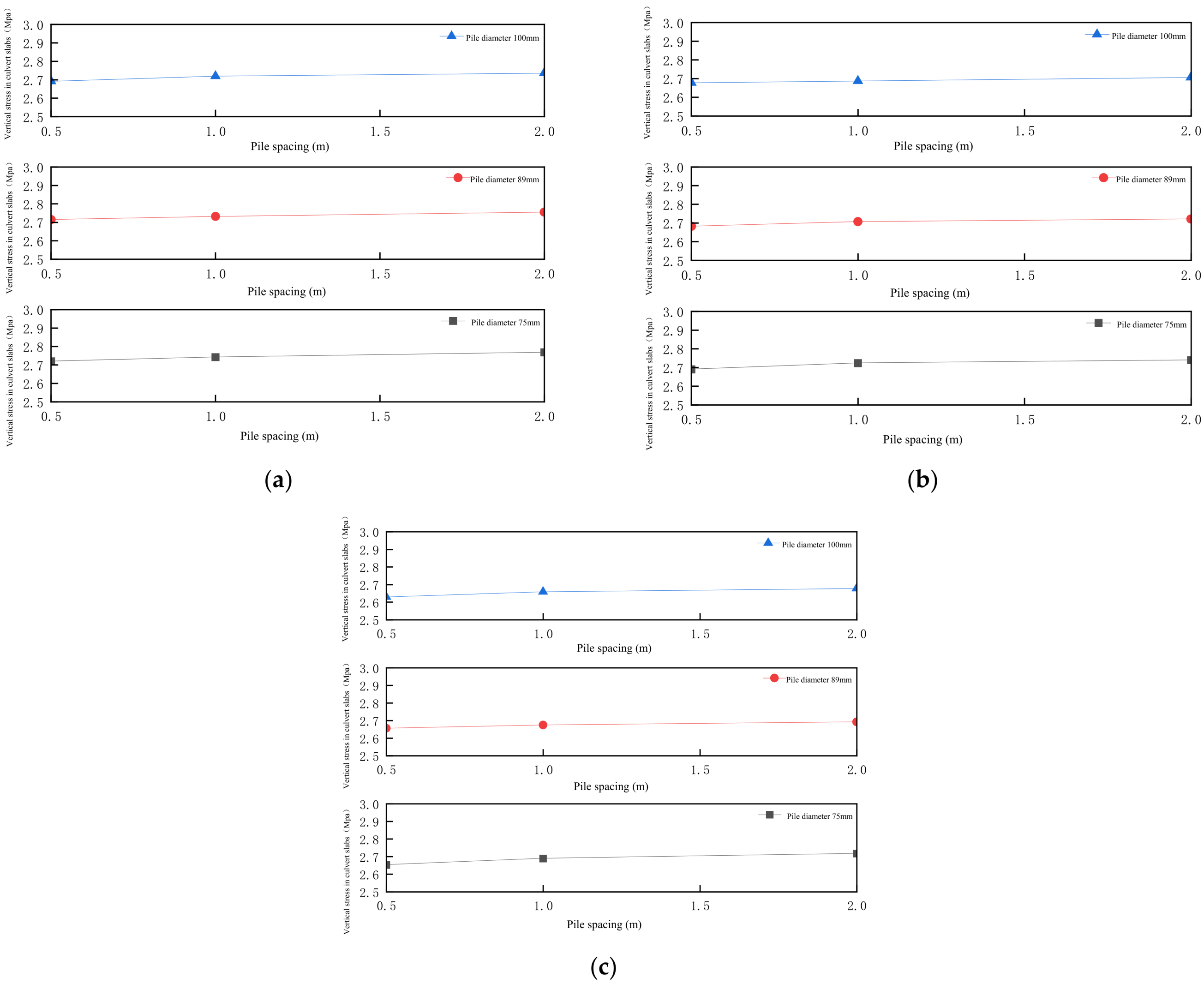

Figure 5. Culvert vertical stress under different pile lengths: (**a**) 0 m; (**b**) 2 m; (**c**) 4 m.

3.3. Simplified Evaluation of Reinforcement Efficiency and Relative Cost

Although detailed economic analysis is beyond the scope of this study, the relationship between reinforcement effectiveness and additional construction input is important for practical engineering applications. Therefore, a simplified relative cost evaluation method is introduced to qualitatively assess the economic efficiency of the proposed reinforcement method.

The total cost can be approximately expressed as:

$$C_r = \alpha V_c + \beta V_s + \gamma n L$$

where C_r denotes the relative reinforcement cost; V_c and V_s denote the volume of additional concrete and reinforcement steel, respectively; n denotes the number of grouted steel pipes; L denotes the length of each pile; and α, β, and γ are the corresponding unit cost coefficients.

Since the material prices and construction expenses vary considerably among different projects, absolute construction costs are not considered in this study. Instead, only the variation trend of reinforcement input is evaluated. For the parametric analysis of pile length, the pile diameter and pile spacing remain unchanged; therefore, the pile-related cost approximately increases proportionally with pile length.

4. Field Tests and Engineering Application

4.1. Project Overview

As a major north–south corridor in China's national highway network, the Beijing–Hong Kong–Macao Expressway also serves as a key longitudinal corridor of the "one vertical and one horizontal" transportation framework in Hunan Province, playing a vital role in connecting Hunan Province with the Yangtze River Economic Belt and the Guangdong–Hong Kong–Macao Greater Bay Area. The present project involves the widening and reconstruction of the expressway under the fourth general contract section, with a chainage ranging from K1795 + 675 to K1814 + 420. The route passes through Aoshang Town and Liangtian Town from north to south, with a total reconstruction length of 18.745 km. The project is designed as a dual eight-lane expressway with a Highway Class I loading standard. The pavement adopts an asphalt concrete structure, and the bridge design also follows the Highway Class I loading standard.

The widening is mainly carried out along both sides of the existing G4 Expressway. National and provincial trunk roads as well as county and township roads are densely distributed along the reconstruction section, resulting in complex construction conditions. The principal engineering quantities are as shown in Table 3. Subgrade works include 2.017 million m^3 of excavation, 1.897 million m^3 of embankment fill, and 121,000 m^3 of soft foundation treatment. The mainline comprises 16 bridges with a total length of 1601 m and 909 precast T-beams. The culvert structures mainly consist of slab culverts and slab passages. A total of 22 circular pipe culverts with a cumulative length of 705 m and 73 slab culverts and slab passages with a cumulative length of 2070 m are included. The fill height above each culvert has increased due to the widening project. The entire alignment includes two interchanges, namely Shuilong Hub Interchange and Liangtian Interchange, and one service area, namely Suxian Service Area. The total paved area of SMA asphalt pavement is approximately 580,000 m^2.

Table 3. Table of the condition of some culverts.

Reference Number	Culvert Type	New Fill Height (m)
K1795 + 696.4	Covered culvert	2.26
K1796 + 086.9	Covered culvert	1.3
K1800 + 541.4	Covered culvert	1.76
YK1800 + 990.7	Covered culvert	3.02
YK1801 + 171.8	Covered culvert	3.63
YK1801 + 379.7	Covered culvert	4.61
YK1801 + 467.1	Covered culvert	5.82
YK1803 + 293.65	Covered culvert	1.06
K1805 + 810.3	Covered culvert	2
K1806 + 050.0	Covered culvert	3.143
K1806 + 183.5	Covered culvert	3.026
K1807 + 120.4	Covered culvert	1.81
K1807 + 354.1	Covered culvert	2.76
K1807 + 472.4	Covered culvert	1.71
K1807 + 598.4	Covered culvert	2.3
K1809 + 358.6	Covered culvert	3.51
K1809 + 512.6	Covered culvert	3.588
K1809 + 538.5	Covered culvert	3.395
K1807 + 490.3	Covered culvert	1.807
K1809 + 807.6	Covered passage	1.024

4.2. Field Tests

To determine the elastic foundation coefficient of the embankment fill above the original culvert, the original pavement is first excavated to the top surface of the fill, followed by a plate load test. The plate load test is an in situ testing method based on the principle that vertical loads are applied incrementally to the foundation soil through a rigid bearing plate at the ground surface or at a predetermined depth, while the corresponding settlement of the plate is measured at each loading level. The plate load tests were conducted in accordance with the Specifications for Geotechnical Test of Highway (JTG 3430–2020) to determine the modulus of subgrade reaction of the composite foundation [23]. The testing apparatus consisted of a circular loading plate, a hydraulic jack, a manual hydraulic pump, a pressure gauge, and high-pressure oil hoses. The loading plate had a diameter of 300 mm, a thickness of 25 mm, and a loading area of 70,650 mm^2, with a positioning mark at its center for the hydraulic jack. The hydraulic jack had a maximum capacity of 100 kN, a stroke of 160 mm, and a lifting height of 100 mm, while the manual hydraulic pump had a rated pressure of 60 MPa. During testing, the loading plate was placed on the leveled test surface, and a loaded truck was positioned with its rear beam directly above the loading plate to provide the reaction force. The hydraulic jack and dial gauges were then installed. To ensure full contact between the loading plate and the ground surface, a seating load of 35 kN was first applied and subsequently released, after which the initial dial gauge reading was taken as the reference settlement. The load was then applied in increments of 10 kN. At each loading stage, the load was maintained until the settlement stabilized, which was defined as a settlement difference of less than 0.01 mm within 1 min, before the settlement was recorded and the next load increment was applied. Loading continued until a maximum load of 90 kN was reached. The measured load–settlement data were subsequently used to determine the modulus of subgrade reaction of the composite foundation.

By analyzing the load–settlement curve, the bearing capacity and deformation characteristics of the foundation soil can be determined. The loading pressure of the plate can be calculated as follows:

$$P_h = \frac{(P_y + P_c - P_f) \cdot S_y}{S_h} \tag{15}$$

where P_h denotes the loading pressure of the plate; S_h denotes the area of the loading plate; P_y denotes the oil pressure inside the jack cylinder; S_y denotes the cylinder area; P_c denotes the pressure acting on the plate due to the self-weight of the jack and the platen; and P_f denotes the pressure on the plate induced by hydraulic circuit losses and piston resistance.

The coefficient of subgrade reaction can be calculated by Equation (16):

$$K = \frac{P_h}{s} \tag{16}$$

Three monitoring sections were selected for this test, located at chainages K1814 + 107, K1814 + 258, and K1814 + 330, respectively. Plate load tests were conducted at each section after removing the original asphalt pavement, reinforced concrete slab, and cement-stabilized crushed stone layer, as shown in Figure 6.

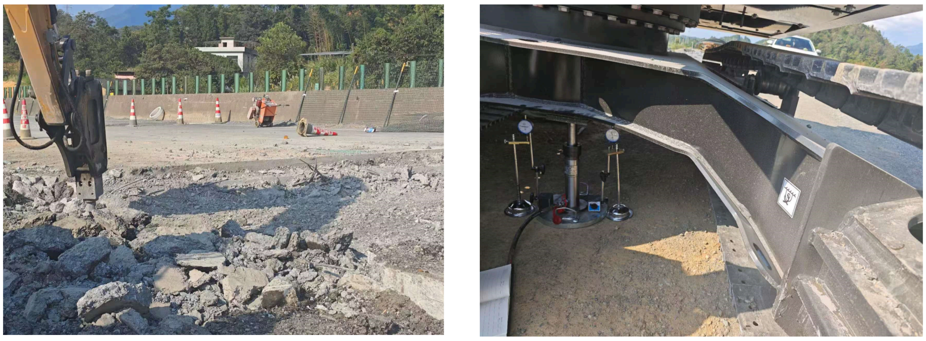

Figure 6. Plate load test.

The measured coefficient of subgrade reaction of the original foundation is presented in Table 4.

Table 4. Subgrade coefficient for the existing foundation.

Culvert	Monitoring Location 1 (K1814 + 107)	Monitoring Location 2 (K1814 + 258)	Monitoring Location 3 (K1814 + 330)
Base bed coefficient (MPa/m)	71.942	66.698	63.215
Average value		67.285	

To further investigate the effects of pile length, pile spacing, and grouting process on the coefficient of subgrade reaction, two culverts were selected for field testing, with test sections located at K1807 + 490.27 and K1807 + 598.395, respectively. A total of 11 groups of grouted steel pipe piles with varying parameters were arranged on both sides of each culvert, and plate load tests were conducted to determine the coefficient of subgrade reaction. As shown in Table 5, the test conditions include three pile lengths: terminating at the culvert base slab, extending 2 m below the culvert base slab, and extending 4 m below the culvert base slab; three pile spacings of 0.5 m, 1 m, and 2 m; and a uniform pile diameter of 89 mm. Under these conditions, no pressure grouting was adopted to investigate the influence of geometric parameters on the bearing capacity of the composite foundation. In addition, to evaluate the enhancement effect of pressure grouting, an additional comparison case was considered, with the pile length extending 2 m below the culvert base slab, pile spacing of 2 m, pile diameter of 89 mm, and grouting pressure ranging from 0.5 to 0.8 MPa.

Table 5. Test conditions for composite foundations.

	Pile Length (m)	Pile Spacing (m)	Pressure Grouting Required	Pile Diameter (mm)
1	terminating at the culvert base slab	2	NO	89
2	extending 2 m below the culvert base slab			
3	extending 4 m below the culvert base slab			
4	terminating at the culvert base slab	1		
5	extending 2 m below the culvert base slab			
6	extending 4 m below the culvert base slab			
7	terminating at the culvert base slab	0.5		
8	extending 2 m below the culvert base slab			
9	extending 4 m below the culvert base slab			
10	extending 2 m below the culvert base slab	0.266		
11	extending 2 m below the culvert base slab	2	Yes	

To ensure the reliability of the test results, nine grouted steel pipe piles were arranged under each condition, and the coefficient of subgrade reaction was measured only at the center of each test section. For each test condition, three plate load tests were performed. The coefficient of subgrade reaction presented in Table 6 represents the average of the three readings, which was calculated to minimize the effects of random measurement errors. The results indicate that the coefficient of subgrade reaction increases as pile length increases and pile spacing decreases, which is consistent with numerical simulation results. In addition, pressure grouting significantly improves the coefficient of subgrade reaction and enhances the reinforcement performance.

Table 6. Foundation bed coefficients for composite foundations.

Operating Condition Number	Description of Operating Condition	Base Bed Coefficient MPa/m	SD	CV (%)
1	Pile spacing 2 m, pile length terminating at the culvert base slab	123.52	5.163	4.18
2	Pile spacing 2 m, pile length extending 2 m below the culvert base slab r	128.31	5.569	4.34
3	Pile spacing 2 m, pile length extending 4 m below the culvert base slab	132.44	4.834	3.65
4	Pile spacing 1 m, pile length terminating at the culvert base slab	127.73	5.114	4.00
5	Pile spacing 1 m, pile length extending 2 m below the culvert base slab	131.35	3.614	2.75
6	Pile spacing 1 m, pile length extending 4 m below the culvert base slab	136.59	2.370	1.73
7	Pile spacing 0.5 m, pile length terminating at the culvert base slab	130.96	3.242	2.48
8	Pile spacing 0.5 m, pile length extending 2 m below the culvert base slab	134.43	5.771	4.29
9	Pile spacing 0.5 m, pile length extending 4 m below the culvert base slab	140.54	6.216	4.42
10	Pile spacing 0.266 m, pile length extending 2 m below the culvert base slab	142.74	5.773	4.04
11	Pile spacing 2 m, pile length extending 2 m below the culvert base slab	137.75	5.683	4.09

4.3. Engineering Application

The midspan deflection of the additional deck slab was obtained using the elastic foundation beam model. The coefficient of subgrade reaction in the pile-reinforced zone and the midspan zone, k_1 and k_2, respectively, differ and were determined based on field test data. Considering the safety factor, the deflection control equation is expressed in Equation (17).

$$1.2k\omega \leq 20000 \tag{17}$$

Taking culvert K1809 + 358.6 as an example, the design parameters of the additional deck slab were determined. The culvert is a 3 m × 3 m slab culvert, with original and additional fill heights of 8.53 m and 3.51 m, respectively. The parameter values are listed in Table 7.

Table 7. Table of Calculation Parameter Values.

Original Fill Height	**8.53 m**	**New Fill Height**	**3.51 m**
Length of the elastic foundation beam above the culvert	4 m	Length of elastic foundation beams on both sides of the culvert	2 m
Subgrade coefficient of the soil above the culvert	67.29 MPa/m	Subgrade modulus of elastic foundation beams on both sides of the culvert	135 MPa/m
Fill density	2000 kg/m^3	Concrete density	2500 kg/m^3
Density of light-weight soil	667 kg/m^3	New pavement density	2200 kg/m^3
Thickness of the new pavement	0.82 m	Modulus of elasticity of concrete	30,000 MPa
Distance between the inner piles and the culvert	0.5 m		

The governing equation was implemented in Python 3.9 to determine the required deck slab thickness. The results indicate that, for a pile spacing of 1 m and a pile length extending 4 m below the culvert base slab, the required deck slab thickness is 44.8 cm. Accordingly, a deck slab thickness of 45 cm was adopted for the engineering design. During the engineering design process, the additional deck slab was further designed and verified in accordance with the applicable structural design codes, including checks for flexural capacity, shear capacity, punching shear, crack control, reinforcement detailing, and the relevant serviceability and ultimate limit states. As these calculations follow established engineering design procedures, the detailed verification process is not presented here. A comparison between the original culvert under the existing embankment and the reinforced culvert after embankment raising shows that the midspan stress decreases from 7.01 MPa to 6.88 MPa, despite an additional embankment height of 3.51 m. These results demonstrate that the proposed reinforcement system effectively redistributes the additional embankment load through the additional deck slab and the composite foundation, thereby reducing the structural demand on the existing culvert. Accordingly, for the investigated engineering conditions, a reinforcement scheme comprising a 45 cm thick additional deck slab and a pile spacing of 1 m is recommended.

5. Conclusions

This study proposed a reinforcement method for existing slab culverts subjected to increased embankment loads in highway widening projects by integrating an additional deck slab with a grouted steel pipe pile-supported composite foundation. A segmented elastic foundation beam model was established to derive the analytical solution for slab deflection and calculate the load acting on the culvert roof. The reinforcement mechanism was further investigated through finite element analysis and field tests. The main conclusions are summarized as follows:

(1) A segmented Winkler foundation beam model was developed to characterize the interaction among the additional deck slab, composite foundation, and existing culvert. The proposed analytical model provides an effective approach for calculating the load acting on the culvert roof and offers a theoretical basis for reinforcement design.
(2) Parametric analyses demonstrated that the reinforcement performance is significantly influenced by pile arrangement, pile diameter, pile length, and pile spacing. Culvert displacement and stress decrease with reduced pile spacing and increased pile diameter and pile length. Within the investigated parameter range, the most favorable reinforcement performance was obtained when the pile length extended 4 m below the culvert base slab.
(3) Field plate load tests showed that the stiffness of the composite foundation increases with increasing pile length and decreasing pile spacing. Pressure grouting further improved the subgrade modulus by approximately 7–10%, indicating that grouting is effective in enhancing the stiffness of the composite foundation.
(4) Based on the analytical model, finite element simulations, and field test results, a set of recommended reinforcement parameters was proposed for culvert K1809 + 358.6, providing practical guidance for reinforcement design in highway widening projects. The proposed method offers the advantages of rapid construction, controllable cost, and minimal traffic disruption.

It should be noted that the recommended pile length extending 4 m below the culvert base slab represents the most favorable solution among the investigated parameter combinations rather than a globally optimal solution. The recommended reinforcement parameters were identified within the investigated parameter range, and a comprehensive multi-objective optimization considering structural performance, construction cost, material consumption, and constructability was beyond the scope of the present study.

Despite these encouraging results, several limitations should be acknowledged. First, the proposed analytical model is based on the Winkler foundation assumption, while the numerical model considers nonlinear behavior only for the soil using the Mohr–Coulomb constitutive model; the concrete and steel components were modeled as linear-elastic materials. Second, the finite element analysis was performed for the final reinforced configuration under service conditions, and the construction sequence—including pavement removal, pile installation, pressure grouting, construction of the additional deck slab, backfilling, and subsequent traffic loading—was not explicitly simulated. Third, although the analytical model, finite element simulations, and field plate load tests consistently support the effectiveness of the proposed reinforcement method, a direct quantitative comparison among these approaches remains limited because the field investigation focused on determining the modulus of subgrade reaction of the composite foundation rather than measuring structural responses such as culvert displacement and stress. Therefore, the analytical, numerical, and field investigations should be regarded as complementary forms of validation rather than directly comparable datasets. Although three plate load tests were conducted for each test condition and the reported values represent the average of the repeated measurements, the limited number of repetitions did not permit a comprehensive statistical assessment of measurement uncertainty.

The proposed reinforcement method was demonstrated through a representative highway widening project and is therefore considered applicable to reinforced concrete slab culverts with similar structural dimensions, embankment heights, foundation conditions, and loading characteristics. For projects involving substantially different culvert sizes, soft or highly heterogeneous soils, exceptionally high embankments, or heavy traffic loads, the reinforcement parameters should be determined through project-specific analysis and verification.

Compared with conventional reinforcement methods using only an additional deck slab or only foundation improvement, the proposed method integrates load redistribution with foundation strengthening, providing a more comprehensive reinforcement strategy. This improvement is achieved at the expense of additional pile installation and pressure grouting, which inevitably increase construction complexity and cost. Therefore, the recommended reinforcement parameters represent the most favorable solution among the investigated cases in terms of structural performance, while the final design should also consider project-specific economic and constructability requirements.

In addition to the single-factor parametric study, a multi-variable numerical analysis involving 27 representative parameter combinations was performed to evaluate potential interaction effects among pile length, pile diameter, and pile spacing. The results indicate that each parameter exhibits a dominant independent influence on the structural response, whereas their interaction effects are relatively weak within the investigated parameter range. This finding supports the applicability of the single-factor analysis for practical parameter selection under the considered engineering conditions. Nevertheless, more comprehensive multi-factor optimization covering a wider range of structural configurations and loading conditions is still warranted. Future research will focus on incorporating more advanced soil constitutive models, simulating staged construction processes and long-term soil–structure interaction, conducting full-scale field monitoring under different engineering conditions, and performing broader multi-factor optimization with uncertainty quantification while simultaneously considering structural performance, construction cost, and constructability.

Author Contributions: Conceptualization, Z.J. and Y.S.; methodology, J.N. and H.C.; software, J.N. and H.C.; validation, Z.J. and Y.S.; formal analysis, Z.J. and Y.S.; investigation, Y.S., J.N. and H.C.; resources, Z.J. and Y.S.; data curation, J.N. and H.C.; writing—original draft preparation, J.N. and Z.J.; writing—review and editing, Z.J. and Y.S.; visualization, H.C.; supervision, Z.J. and Y.S.; project administration, Y.S.; funding acquisition, Z.J. All authors have read and agreed to the published version of the manuscript.

Funding: This research received no external funding.

Institutional Review Board Statement: Not applicable.

Informed Consent Statement: Not applicable.

Data Availability Statement: The data sets used or analysed in this study are available from the corresponding author upon reasonable request.

Acknowledgments: The author would like to express gratitude to Guangxi Jiaojian Engineering Construction Group Co., Ltd., for their support with the on-site trials.

Conflicts of Interest: Author Zhijie Jiang was employed by the company Guangxi Jiaojian Engineering Construction Group Co., Ltd. The remaining authors declare that the research was conducted in the absence of any commercial or financial relationships that could be construed as a potential conflict of interest.

References

1. Zeyrek, O.; Wang, F.; Xu, J. Behaviors of Highway Culverts Subjected to Flooding: A Comprehensive Review. *Water* **2025**, *17*, 2937. [CrossRef]
2. Hwang, B.-G.; Zhao, X.; Ng, S.Y. Identifying the Critical Factors Affecting Schedule Performance of Public Housing Projects. *Habitat Int.* **2013**, *38*, 214–221. [CrossRef]

3. Liu, H.; Pan, Y.; Gao, X.; Hu, S. Vertical Load on Embankment-Installed Rigid Culvert Buried by Cohesionless Fill. *Transp. Geotech.* **2026**, *57*, 101898. [CrossRef]
4. Simpson, B.; Hoult, N.A.; Moore, I.D. Rehabilitated Reinforced Concrete Culvert Performance under Surface Loading. *Tunn. Undergr. Space Technol.* **2017**, *69*, 52–63. [CrossRef]
5. Beben, D.; Stryczek, A. Numerical Analysis of Corrugated Steel Plate Bridge with Reinforced Concrete Relieving Slab. *J. Civ. Eng. Manag.* **2015**, *22*, 585–596. [CrossRef]
6. Huynh, A.; Petit, B.; Téply, F.; Larive, C. Innovative Rehabilitation Technology for Corrugated Metal Pipe Culverts Using Wet-Mix Sprayed UHPFRC. In *Proceedings of the International Symposium on Ultra-High Performance Fibre-Reinforced Concrete (UHPFRC 2017), Montpellier, France, 2–4 October 2017*; Toutlemonde, F., Resplendino, J., Eds.; RILEM Publications SARL: Paris, France, 2017; pp. 717–723.
7. Lassy, B.; Hain, A. Evaluation of Construction Methods for Ultra-High Performance Concrete Invert Linings in Corrugated Metal Pipe Culverts. *Infrastructures* **2025**, *10*, 322. [CrossRef]
8. Jin, J.; Su, M.; Lang, K.; Zhang, H.; Ye, X.; Shi, W. Load-Bearing Behavior of Pipe-Arch Corrugated Steel Pipes during Backfilling. *J. Struct. Eng.* **2025**, *151*, 04025175. [CrossRef]
9. Yoo, D.-Y.; Banthia, N. Mechanical Properties of Ultra-High-Performance Fiber-Reinforced Concrete: A Review. *Cem. Concr. Compos.* **2016**, *73*, 267–280. [CrossRef]
10. Chen, B.-G.; Yang, Z.-Z.; Song, D.-B. Long-Term Mechanical Behavior of Load-Shedding Culverts on Soft Soil Foundation. *Tunn. Undergr. Space Technol.* **2026**, *172*, 107558. [CrossRef]
11. Sun, L.; Hopkins, T.C.; Beckham, T.L. Long-Term Monitoring of Culvert Load Reduction Using an Imperfect Ditch Backfilled with Geofoam. *Transp. Res. Rec.* **2011**, *2212*, 56–64. [CrossRef]
12. Xie, M.; Zheng, J.; Dong, J.; Miao, C. Foundation Improvement with Lattice-Shaped Diaphragm Wall Treatment for High Embankment Culverts on Soft Foundation. *Tunn. Undergr. Space Technol.* **2020**, *104*, 103535. [CrossRef]
13. Fernando, N.S.M.; Small, J.C.; Carter, J.P. Elastic Analysis of Buried Structures Subject to Three-Dimensional Surface Loading. *Int. J. Numer. Anal. Methods Geomech.* **1996**, *20*, 331–349. [CrossRef]
14. Ramadan, S.H.; El Naggar, M.H. Field Monitoring and Numerical Analysis of Large-Span Three-Sided Reinforced Concrete Culvert. *J. Geotech. Geoenviron. Eng.* **2021**, *147*, 04021008. [CrossRef]
15. Bian, X.; Tang, X.; Shen, W.; Ling, D.; Chen, Y. An Experimental Study on a Culvert Buried in Granular Soil Subjected to Vehicle Loads. *Adv. Struct. Eng.* **2012**, *15*, 1031–1040. [CrossRef]
16. Huang, H.; Chen, X.; Liu, J.; Chen, Q. A Theoretical Calculation Method of Irregular Bridge Span Pontoon Connected by Elastic Hinges. *Mar. Struct.* **2021**, *76*, 102929. [CrossRef]
17. Zhang, Q.; Deng, H.; Yi, W.; Dai, G.; Li, H.; Guo, X. Study on Uplift Mechanism of Grouted Implantation Steel Pipe Pile by Direct Shear and Model Tests. *Soils Found.* **2024**, *64*, 101459. [CrossRef]
18. Wang, X.; Mao, Z.; Wang, W. Digital Evaluation of Vertical Compressive Bearing Capacity for Jet Grouting Pile–Mini Steel Pipe Pile Composite Foundation. *Math. Probl. Eng.* **2022**, *2022*, 8499597. [CrossRef]
19. Zhang, B.; Hou, H.; Wang, J.; Zhang, S.; Zhao, Y. Comparative Investigation of Axial Monotonic Performance of Grouted Helical Steel Pipe Piles (GHSPP): Experiments, Simulations and Calculation Method. *Structures* **2024**, *70*, 107783. [CrossRef]
20. *GB/T 50783-2012*; Technical Code for Composite Foundation. China Planning Press: Beijing, China, 2012.
21. *GB 50010-2010 (2015 Edition)*; Code for Design of Concrete Structures. China Architecture & Building Press: Beijing, China, 2015.
22. *GB 50017-2017*; Standard for Design of Steel Structures. China Planning Press: Beijing, China, 2017.
23. *JTG 3430-2020*; Specifications for Geotechnical Test of Highway. China Communications Press Co., Ltd.: Beijing, China, 2020.